Journal of Materials Chemistry

PAPER

3,6-Di(furan-2-yl)pyrrolo[3,4-c]pyrrole-1,4(2H,5H)-dione and bithiophene copolymer with rather disordered chain orientation showing high mobility in organic thin film transistors†

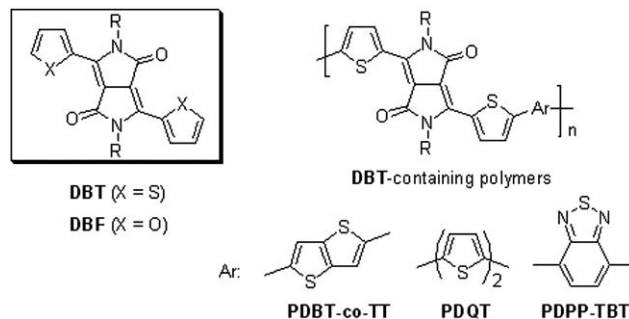Yuning Li,*[ab] Prashant Sonar,[b] Samarendra P. Singh,[b] Wenjin Zeng[b] and Mui Siang Soh[b]

Pyrrolo[3,4-c]pyrrole-1,4(2H,5H)-dione or diketopyrrolopyrrole (DPP) is a useful electron-withdrawing fused aromatic moiety for the preparation of donor–acceptor polymers as active semiconductors for organic electronics. This study uses a DPP-furan-containing building block, 3,6-di-(furan-2-yl)pyrrolo[3,4-c]pyrrole-1,4(2H,5H)-dione (DBF), to couple with a 2,2′-bithiophene unit, forming a new donor–acceptor copolymer, PDBFBT. Compared to its structural analogue, 3,6-di-(thiophen-2-yl)pyrrolo[3,4-c]pyrrole-1,4(2H,5H)-dione (DBT), DBF is found to cause blue shifts of the absorption spectra both in solution and in thin films and a slight reduction of the highest occupied molecular orbital (HOMO) energy level of the resulting PDBFBT. Despite the fact that its thin films are less crystalline and have a rather disordered chain orientation in the crystalline domains, PDBFBT shows very high hole mobility up to 1.54 cm² V⁻¹ s⁻¹ in bottom-gate, top-contact organic thin film transistors.

Introduction

Pyrrolo[3,4-c]pyrrole-1,4(2H,5H)-dione or diketopyrrolopyrrole (DPP) has recently become a popular conjugated moiety incorporated in polymer semiconductors[1] for organic light-emitting diodes (OLEDs),[2,3] organic thin film transistors (OTFTs),[4–9] and organic photovoltaics (OPVs).[10–15] Due to its strong electron withdrawing effect, DPP could reduce the lowest unoccupied molecular orbital (LUMO) energy level of the resulting polymers. Donor–acceptor polymers of DPP coupled with other proper moieties exhibit interesting ambipolar transport properties, *i.e.*, conducting both electrons and holes, making them useful as channel semiconductors in ambipolar OTFTs for fabricating CMOS-like circuits.[4,6,9,14,15] They also show excellent performance in OPV devices owing to their high hole mobility for efficient charge transport as well as their optimum band gaps for light harvesting.[10–15] The DPP-containing building block, 3,6-di-(thiophen-2-yl)pyrrolo[3,4-c]pyrrole-1,4(2H,5H)-dione (DBT, Fig. 1), can be readily synthesized and is particularly useful for constructing conjugated polymers for OTFTs and OPVs.[4–9,14,15]

The two thiophene units adjacent to DPP can alleviate their steric repulsions with DPP to maintain high coplanarity of the polymer backbone, which is essential for achieving efficient charge transport properties and low band gaps.

Recently, we designed several DBT-based donor–acceptor polymers, *e.g.*, PDBT-*co*-TT,[7] PDQT,[8] and PDPP-TBT[9] (Fig. 1), which showed high hole mobility up to ∼1 cm² V⁻¹ s⁻¹ in p-channel OTFT devices[7,8] and balanced high electron (∼0.40 cm² V⁻¹ s⁻¹) and hole (∼0.35 cm² V⁻¹ s⁻¹) mobilities in ambipolar OTFT devices.[9] Until recently, furan has been paid much less attention compared to thiophene and very few furan-containing oligomers and polymers have been reported for OTFT

[a] Department of Chemical Engineering and Waterloo Institute for Nanotechnology (WIN), University of Waterloo, 200 University Ave West, ON, Canada N2L 3G1. E-mail: yuning.li@uwaterloo.ca; Fax: +1 15198884347; Tel: +1 1-519-888-4567 ext. 31105
*[b] Institute of Materials Research and Engineering (IMRE), Agency for Science, Technology, and Research (A*STAR), 3 Research Link, Singapore, 117602*
† Electronic supplementary information (ESI) available: NMR, MODI-TOF MS, and DSC data of compounds **1**–**3** and PDBFBT. See DOI: 10.1039/c1jm11290b

Fig. 1 Structures of 3,6-di(thiophen-2-yl)pyrrolo[3,4-c]pyrrole-1,4-(2H,5H)-dione (DBT), 3,6-di(furan-2-yl)pyrrolo[3,4-c]pyrrole-1,4-(2H,5H)-dione (DBF) building blocks, and representative DBT-containing polymers, PDBT-*co*-TT,[7] PDQT,[8] and PDPP-TBT,[9] for OTFTs.

This journal is © The Royal Society of Chemistry 2011

J. Mater. Chem., 2011, **21**, 10829–10835 | 10829

applications.[16–21] In this study, we use the furan-containing 3,6-di-(furan-2-yl)pyrrolo[3,4-c]pyrrole-1,4(2H,5H)-dione (DBF, Fig. 1), a structural analogue of DBT, to synthesize a donor–acceptor alternating copolymer, PDBFBT (Scheme 1). A few DBF-containing polymers were reported very recently, which showed good photovoltaic performance in OPVs.[20,21] Our results in this work demonstrate that the DBF building block could also be potentially very useful for high performance polymer semiconductors in OTFTs.
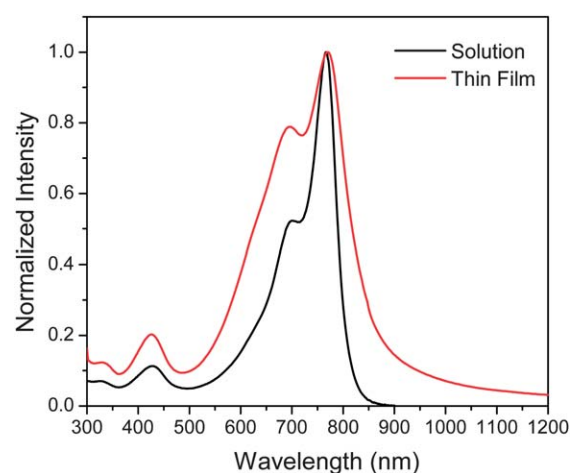
Results and discussion

The DBF-bithiophene alternating copolymer, PDBFBT, was synthesized according to Scheme 1. The DBF core, 3,6-di(furan-2-yl)pyrrolo[3,4-c]pyrrole-1,4(2H,5H)-dione (1), was prepared in 61% yield by reacting 2-furylnitrile with diisopropyl succinate in the presence of sodium 2-methyl-2-butanoate in accordance to a similar procedure for the preparation of 3,6-di(thiophen-2-yl)-pyrrolo[3,4-c]pyrrole-1,4(2H,5H)-dione (DBT).[5,7] Substitution at nitrogen atoms with an alkyl side chain, 2-octyldodecyl, using 2-octyldodecyl bromide in the presence of potassium carbonate and the subsequent bromination at the α-position of furan units using bromine (Br$_2$) afforded 2,5-bis(2-octyldodecyl)-3,6-di-(furan-2-yl)pyrrolo[3,4-c]pyrrole-1,4(2H,5H)-dione (2) (48% yield) and 3,6-bis(5-bromofuran-2-yl)-2,5-bis(2-octyldodecyl)-pyrrolo[3,4-c]pyrrole-1,4(2H,5H)-dione (3) (58% yield), respectively. Stille coupling polymerization of 3 with 5,5′-bis-(trimethylstannyl)-2,2′-bithiophene formed the target polymer PDBFBT, which was purified using Soxhlet extraction successively with acetone and hexane, yielding a dark solid (~99%). PDBFBT showed excellent solubility in several common solvents including chloroform, toluene, and tetrahydrofuran (THF) at room temperature. The number average molecular weight (M_n) and polydispersity index (PDI, M_w/M_n) of PDBFBT were determined to be 130 500 and 2.27 by using gel permeation chromatography (GPC) at a column temperature of 40 °C with THF as an eluent and polystyrene as standards.

PDBFBT in chloroform exhibits the maximum absorption (λ_{max}) at 770 nm along with one shoulder at 700 nm (Fig. 2). In the solid thin film, PDBFBT shows only a slight red-shift of 6 nm in λ_{max} (776 nm), but the absorption profile is broadened compared to its solution absorption spectrum. The optical band gap of the polymer thin film is calculated from the absorption cut-off (~880 nm) to be 1.41 eV. It was observed previously that
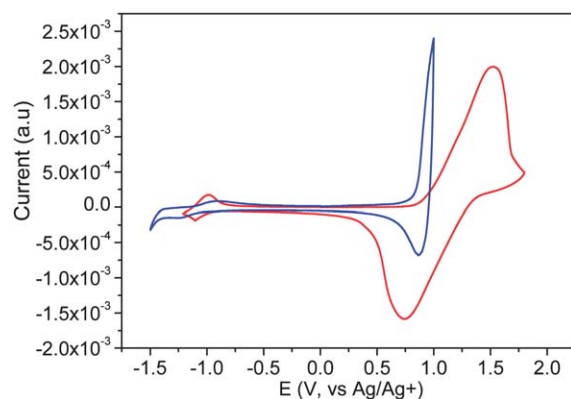

**Fig. 2** UV-vis-NIR absorption spectra of PDBFBT in chloroform and in thin film.

PDQT, the structural analogue of PDBFBT, showed a longer λ_{max} (777 nm in chloroform; 790 nm in thin films) and a smaller band gap (1.24 eV).[8] Experimental and theoretical data have shown that polyfuran has a wider band gap (~2.35 eV) than that (~2.00 eV) of polythiophene.[22] Our results are in good agreement with this trend, showing that the introduction of furan units indeed has broadened the optical band gap of PDBFBT (Fig. 2).

Electrochemical measurements of PDBFBT thin films with cyclic voltammetry (CV) show a reversible oxidative process (Fig. 3). The highest occupied molecular orbital (HOMO) energy level was determined from the oxidation onset potential (~0.92 V) to be 5.32 eV, which is lower than that (5.20 eV) of PDQT. The reductive process of PDBFBT is also reversible, but the currents are significantly lower compared to the oxidative process. The LUMO level of PDBFBT was estimated to be 3.91 eV from its optical band gap and HOMO level.

Thermal properties of PDBFBT were characterized using differential scanning calorimetry (DSC). PDBFBT shows an endothermic peak at 286 °C during the first heating scan and an exothermic peak at 253 °C during the subsequent cooling, which

Scheme 1 Synthesis of PDBFBT: (i) t-C$_5$H$_{11}$OK/2-methyl-2-butanol/ 120 °C; (ii) K$_2$CO$_3$/DMF/130 °C; (iii) chloroform/Br$_2$/rt; (iv) Pd (PPh$_3$)$_2$Cl$_2$/toluene/90 °C.

Fig. 3 Cyclic voltammograms of a PDBFBT thin film (red lines) and a PDQT[8] thin film (blue lines) showing the first oxidative and reductive cycles at a scan rate of 100 mV s^{-1}. The electrolyte was 0.1 M tetrabutylammonium hexafluorophosphate in anhydrous acetonitrile.
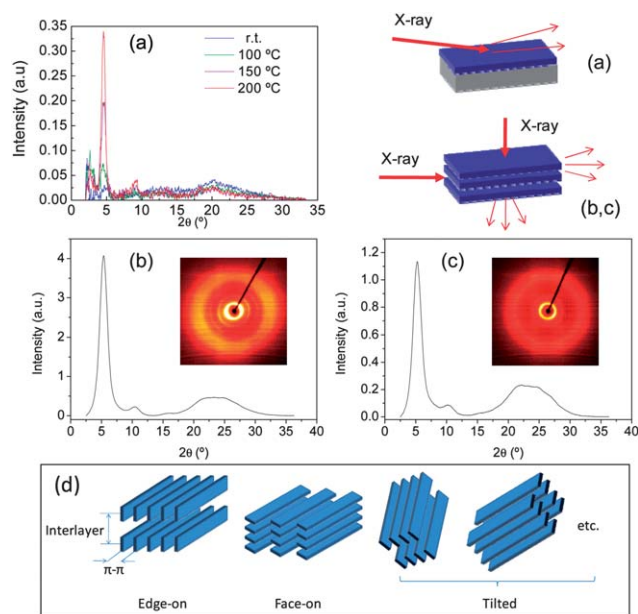
Fig. 4 XRD diffraction patterns of PDBFBT thin films annealed at different temperatures on Si/SiO$_2$ substrates (a) and a stack of PDBFBT thin films (annealed at 200 °C under nitrogen for 15 min) with the incident X-ray parallel (b) and perpendicular (c) to the thin films. Insets in (b) and (c) are 2-D XRD images obtained with the incident X-ray parallel and perpendicular to the film stacks. (d) Illustrates the possible lamellar crystalline domains with edge-on, face-on, and tilted chain orientations in the polymer thin films.

correspond to the melting and crystallization temperatures of this polymer, respectively (see ESI†).

Molecular organization of PDBFBT was studied using X-ray diffractometry (XRD) measurements on polymer thin films. A heavily n-doped silicon wafer with a ~200 nm thermally grown SiO$_2$ layer on top was used as the substrate. Prior to use, the surface of the SiO$_2$ layer was treated with octyltrichlorosilane (OTS) to form a monolayer of octyl groups on the surface, which could improve the interfacial properties of the substrate with the subsequently coated polymer semiconductor layer and might facilitate the establishment of an edge-on molecular packing motif of the polymer chains.[23] As shown in Fig. 4a, the as-spun thin film exhibits a broad diffraction peak around $2\theta = {\sim}20°$ ($d = {\sim}4.4$ Å), indicating the amorphous nature of this sample. Upon annealing at 100 °C, a diffraction peak at 4.56° appears. As the annealing temperature increased further to 150 and 200 °C, this primary diffraction peak becomes intensified, but the broad peak around $2\theta = {\sim}20°$ remains. Based on the previous studies on PDQT[8] and many other crystalline conjugated polymers,[24–28] the polymer chains in the annealed crystalline PDBFBT thin films likely adopt a layer-by-layer lamellar packing manner. The peak at $2\theta = 4.56°$ corresponds to a d-spacing of 19.4 Å of the crystalline lamellae. These thin film XRD results indicate that PDBFBT in the as-spun and annealed thin films is less crystalline compared to its DBT-containing polymer analogue, PDQT.[8] To further elucidate the molecular organization, two-dimensional (2-D) transmission XRD measurements were carried out on a stack of polymer thin films (annealed at 200 °C for 30 min prior to measurements), with the

incident X-ray parallel and perpendicular to the polymer thin films, respectively (Fig. 4). The diffraction patterns obtained with the parallel and perpendicular X-ray irradiation modes are similar (Fig. 4b and c), unlike PDQT which showed dramatically different diffraction patterns with different X-ray irradiation modes.[8] The broad featureless diffractions from $2\theta = 17$ to 32° are probably contributed from both the short range order of the amorphous regions and the π–π stacking distance of the crystalline domains in the polymer thin films. The intensity ratio (~8.9) of the primary peak to the broad peak at $2\theta = {\sim}23°$ obtained with the parallel X-ray mode (Fig. 4b) is slightly higher than that (~5.9) obtained with a perpendicular X-ray mode (Fig. 4c). The limited enhancement in the diffraction at $2\theta = {\sim}23°$ observed with the X-ray perpendicular to the thin film (Fig. 4c) might imply that the polymer chains in the thin films have a slight preference in the edge-on orientation, but the face-on and other tilted chain orientations likely co-exist (Fig. 4d).

The morphologies of PDBFBT thin films spin-coated on OTS-modified Si/SiO$_2$ substrates were examined with atomic force microscopy (AFM). The AFM height and phase images are shown in Fig. 5 and 6, respectively. The as-spun thin film without thermal annealing shows a uniform surface with very fine domains. As the annealing temperature increased to 100 °C, large domains appear in the AFM height image, but the phase image remains uniform. When the annealing temperature increased to 150 °C, worm-like fibrils start to appear in both the height and phase images. The polymer thin film annealed at a further elevated temperature of 200 °C is composed of nanometre-sized grains (~10's nm in diameter), which are presumably due to the evolution of crystallization. The thin film morphology (phase images in particular) dependence on the annealing temperature agrees well with the changes in crystallinity of the thin films upon thermal annealing observed with XRD (Fig. 4a).
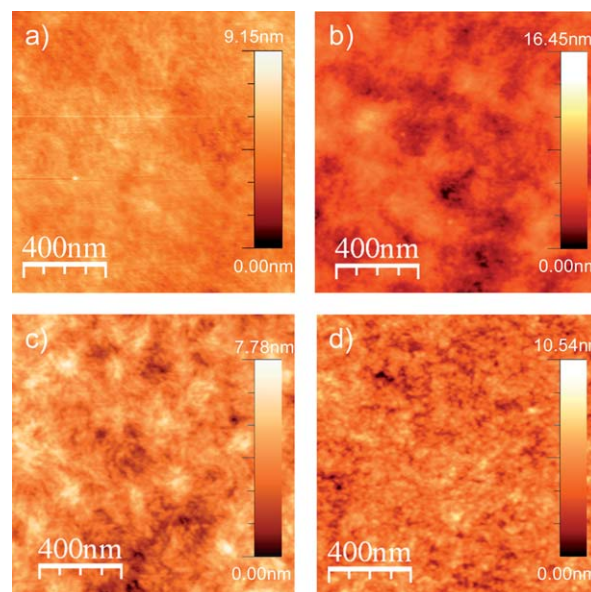
Fig. 5 AFM height images of a PDBFBT thin film (~30 nm) without annealing (a) and annealed at 100 (b), 150 (c), and 200 °C (d) for 15 min under nitrogen.
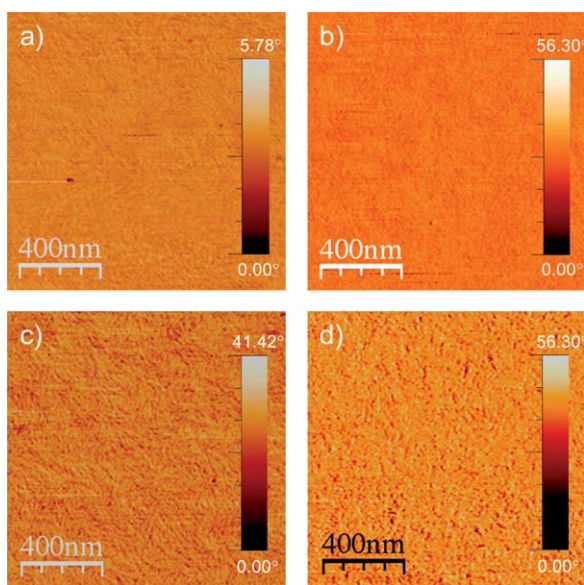
Fig. 6 AFM phase images of a PDBFBT thin film (∼30 nm) without annealing (a) and annealed at 100 (b), 150 (c), and 200 °C (d) for 15 min under nitrogen.

Field effect transistor performance of PDBFBT as a channel semiconductor was evaluated in OTFT devices with a bottom-gate, top-contact OTFT configuration. A polymer thin film (∼30 nm) was deposited on top of the OTS-modified SiO$_2$/Si substrate by spin coating a polymer solution in chloroform (6 mg mL^{-1}). The polymer thin films were optionally annealed on a hotplate at 100, 150, and 200 °C, respectively, in a glove box filled with nitrogen. Gold thin films were then thermally evaporated on top of the polymer thin film to form source/drain electrode features using a shadow mask. Current–voltage (I–V) characteristics of OTFTs were measured under nitrogen.

As shown in Fig. 7a and b, an OTFT device with a non-annealed polymer thin film displays typical p-type semiconductor characteristics with hole mobility of 0.13 cm^2 V^{-1} s^{-1} in the saturation regime and a current on-to-off ratio (I_{on}/I_{off}) of 1.8 × 10^6. Annealing the polymer thin film at 100, 150, and 200 °C increases the mobility progressively to 0.51, 0.65, and 1.54 cm^2 V^{-1} s^{-1}, respectively, with high current on-to-off ratios maintained at ∼10^6 (Fig. 7c–h). The threshold voltages for all devices are in the range of −3.42 to −5.79 V. Interestingly, the slope of the (I_{DS})$^{1/2}$ vs. V_{GS} curves (and thus the calculated mobility) for all devices decreases as the gate voltage increases. For instance, a mobility of 1.54 cm^2 V^{-1} s^{-1} for the OTFT device with a polymer thin film annealed at 200 °C is calculated from the linear fitting of (I_{DS})$^{1/2}$ with V_{GS} in the range from −8 to −17 V (Fig. 7g). As the gate voltage increases beyond −18 V, the slope of the (I_{DS})$^{1/2}$ vs. V_{GS} curve starts to drop considerably. The mobility calculated in the V_{GS} range from −19 to −39 V is 0.17 cm^2 V^{-1} s^{-1}. This phenomenon is rather unusual, as for most organic semiconductors that show gate-dependent charge transport behaviour, their mobility increases with increasing gate voltage due to the presence of charge traps and structural defects.[29–31] Decreases in mobility as the gate voltage increases were only observed for a few organic semiconductors, e.g., sexithiophene,[32] rubrene,[33] and pentacene,[34] which were
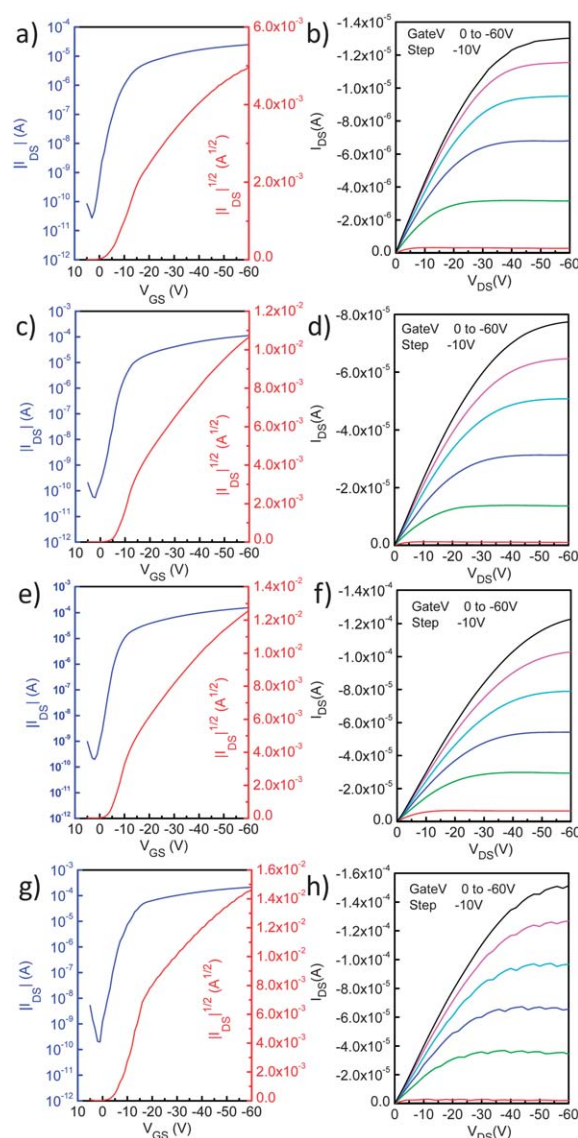
Fig. 7 Output (V_{GS} = 0 V to −60 V) and transfer characteristics of OTFTs with a PDBFBT thin film without annealing (a and b), annealed at 100 °C (c and d), 150 °C (e and f), and 200 °C (g and h) for 15 min under nitrogen (L = 125 μm; W = 4 mm).

attributed to the contact resistance between the semiconductor and the source/drain electrodes.[32] The gate bias dependent mobility observed for PDBFBT is likely related to a non-linear increase of the charge carrier concentration against the increasing gate voltage, which might be originated from (i) the relatively low HOMO level (5.32 eV) of this polymer that poorly matches the work function (∼4.5 ± 0.1 eV)[35] of the gold contacts and/or (ii) the poor interfacial properties of the polymer and the dielectric layers. The polymer thin films annealed at 200 °C showed mobility of 1.02–1.54 cm^2 V^{-1} s^{-1} in the saturation regime among 8 OTFT devices fabricated in two batches. It has been conventionally considered that the establishment of an edge-on chain orientation is favoured for efficient charge transport of conjugated polymers such as P3HT[24] in an OTFT where the charge transport occurs parallel to the dielectric layer. It was only very recently reported that a few polymers with a face-on chain

orientation could also be highly efficient charge transport materials in OTFTs.[36,37] The high charge carrier transport performance observed for PDBFBT having appreciable amorphous regions and without a preferential edge-on chain orientation is rather unexpected. We think the high performance is partially contributed from (i) the strong intermolecular interactions of PDBFBT arisen from the fused DPP rings and the donor (furan and thiophene units)–acceptor (DPP units) interactions and (ii) the well-interconnected thin film morphology.[7,8] The enhanced intermolecular interactions would bring the polymer chains into a close proximity, while the well-interconnected morphology facilitates charge hopping between crystalline domains.

OTFT devices were also characterized in ambient conditions to investigate the air stability of this polymer. It was found that the mobility decreased when the devices were measured in air. However, once the devices were heated and then characterized again in nitrogen, high mobility could be recovered. As shown in Fig. 8, when measured in air, the device (with the PDBFBT thin film pre-annealed at 100 °C in nitrogen) showed a mobility of 0.17 cm^2 V^{-1} s^{-1} in the saturation regime, with a current on-to-off ratio of 3.2×10^6. After the same device was heated at 100 °C for 30 min and then measured again under nitrogen, a high mobility of 0.74 cm^2 V^{-1} s^{-1} and a current on-to-off ratio of 2.0×10^7 were obtained. These results suggest that the drop in mobility in air is not caused by catastrophic photooxidative degradation of the furan units.[38] The observed low mobility of the OTFTs when measured in air is also unlikely due to a reversible oxygen doping mechanism,[39] since PDBFBT possesses an even lower HOMO level (5.32 eV) than that (5.1–5.25 eV) of several polymers[25–28,40] which are stable against oxygen doping. The air sensitivity observed for the PDBFBT OTFT devices is thought to be caused by the physical absorption of water molecules on the polymer thin film, because this polymer is relatively polar due to the nature of donor–acceptor moieties in the conjugated backbone. Heating the air-exposed devices would remove the moisture absorbed on the polymer thin films and restore the device performance.

Conclusions

We have demonstrated that 3,6-di(furan-2-yl)pyrrolo[3,4-c]-pyrrole-1,4(2H,5H)-dione (DBF) is a promising building block for preparing high performance conjugated polymers for OTFTs. The copolymer of DBF with bithiophene, PDBFBT, shows high hole mobility of up to 1.54 cm^2 V^{-1} s^{-1} even though the polymer thin films are less crystalline and rather disordered in the polymer chain orientation. The high field effect transistor performance is considered to be partially originated from its strong intermolecular interactions and the well-interconnected thin film morphology.

Experimental

Instrumentation and materials

NMR data were collected on a Bruker DPX 300 MHz or 400 MHz NMR spectrometer with chemical shifts referenced to tetramethylsilane (TMS). Matrix assisted laser desorption/ionization time-of-flight (MALDI-TOF) mass spectra were obtained on a Bruker Autoflex TOF/TOF. UV-vis-NIR spectra were recorded on a Shimadzu model 2501-PC. Cyclic voltammetry (CV) experiments were performed using an Ecochimie PGSTAT30 Autolab potentiostat in 0.1 M tetrabutylammonium hexafluorophosphate in dry acetonitrile at a scanning rate of 100 mV s^{-1}. An Ag/AgCl in 3 M KCl electrode, a platinum wire, and a platinum foil were used as the reference electrode, counter electrode, and working electrode, respectively. The working electrode was coated with a polymer film using a polymer solution in chloroform. The HOMO energy level was calculated using the equation $E_{HOMO} = E_p' + 4.4$ eV, where E_p' is the onset potential for oxidation relative to the Ag/AgCl reference electrode.[41] Differential scanning calorimetry (DSC) was carried out on a TA Instrument DSC Q100 under nitrogen. X-Ray diffraction patterns of thin films deposited on the octyltrichlorosilane (OTS)-modified Si/SiO$_2$ substrate was obtained with a PANalytical X'PERT PRO system using Cu K$_\alpha$ source ($\lambda = 1.5418$ Å). Two-dimensional (2-D) transmission XRD measurements were carried out similarly as described in ref. 28. The samples for 2-D XRD measurements were prepared by evaporating the solvent from a dilute polymer solution in chloroform to form a thin layer of polymer thin film on the flask, followed by carefully rinsing off the thin film with methanol. The polymer thin film ($\sim$100 nm thick) was then cut into small pieces and stacked ($\sim$100 μm thick) for 2-D XRD measurements. Gel permeation chromatography (GPC) measurements were performed on a Waters 2690 System at a column temperature of 40 °C using tetrahydrofuran as eluent and polystyrene as standards. Fourier-transform infrared (FT-IR) analysis was carried out using a Bio-Rad FTS 3000MX spectrometer. All chemicals were purchased from Sigma-Aldrich and Strem as received. 5,5′-Bis(trimethylstannyl)-2,2′-bithiophene was synthesized according to the literature method.[42]
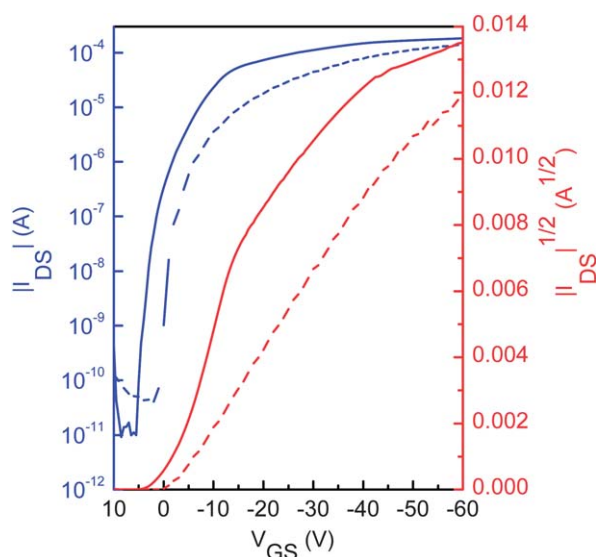
Fig. 8 Transfer ($V_{DS} = -60$ V) characteristics of an OTFT device ($L = 75$ μm; $W = 4$ mm) with a PDBFBT thin film annealed at 100 °C measured in air (dotted lines) and under nitrogen after being re-heated at 100 °C for 30 min (solid lines). The calculated mobility in the saturation regime is 0.17 cm^2 V^{-1} s^{-1} measured in air and 0.74 cm^2 V^{-1} s^{-1} measured under nitrogen after being re-heated.

This journal is © The Royal Society of Chemistry 2011

J. Mater. Chem., 2011, **21**, 10829–10835 | 10833

Synthesis of 3,6-di(furan-2-yl)pyrrolo[3,4-c]pyrrole-1,4(2H,5H)-dione (1)

To a three-necked flask containing 2-methyl-1-butanol (60 mL) was added sodium (3.45 g, 0.15 mol) under argon. The mixture was heated to 90 °C and iron(III) chloride (FeCl₃) (50 mg) was added. After sodium disappeared, the solution was cooled to 85 °C. 2-Furonitrile (9.31 g, 0.10 mol) was added to the reaction mixture, followed by drop-wise addition of diisopropyl succinate (8.1 g, 0.04 mol) in 2-methyl-1-butanol (5 mL) over 1 h at 85 °C. When the addition was completed, the mixture was stirred for additional 2 h at this temperature. The reaction mixture was then cooled to 50 °C, diluted with methanol (50 mL), and then slowly neutralized with glacial acetic acid (~15 mL) and refluxed for 15 min. The reaction mixture was cooled down to room temperature and filtered. The solid was washed respectively with hot methanol and de-ionized (DI) water several times, and dried *in vacuo* at 50 °C for 15 h. A dark red solid was obtained. Yield: 6.54 g (61.0%). ^{1}H NMR (300 MHz, DMSO-d_6): δ 11.17 (s, 2H), 8.04 (d, $J = 1.3$ Hz, 2H), 7.65 (d, $J = 3.4$ Hz, 2H), 6.83 (dd, $J = 1.3$, 3.4 Hz, 2H). ^{13}C NMR (75 MHz, DMSO-d_6): δ 107.57, 113.71, 116.79, 131.27, 143.75, 146.91, 161.71.

Synthesis of 2,5-bis(2-octyldodecyl)-3,6-di(furan-2-yl)pyrrolo-[3,4-c]pyrrole-1,4(2H,5H)-dione (2)

To a dry 250 mL three-neck round bottom flask were added **1** (3.0 g. 11.18 mmol), anhydrous K₂CO₃ (4.63 g, 33.54 mmol), and anhydrous N,N-dimethylformamide (DMF) (250 mL). The mixture was heated to 120 °C under argon for 1 h. 2-Octyldodecylbromide (12.12 g, 33.54 mmol) was then added drop-wise, and the reaction mixture was further stirred overnight at 130 °C. The reaction mixture was allowed to cool down to room temperature and poured into DI water (500 mL) and stirred for 30 min. The product was extracted with chloroform, washed with DI water, and dried over anhydrous MgSO₄. Removal of the solvent afforded the crude product which was further purified using column chromatography on silica gel (a mixture of hexane and chloroform as eluent) to give the product as a red solid (4.5 g, 48%). Mp (DSC): 110.5 °C. ^{1}H NMR (400 MHz, CDCl₃): δ 0.86 (t, $J = 6.4$ Hz, 12H), 1.15–1.40 (m, 64H), 1.79 (s, 2H), 4.01 (m, 4H), 6.68 (dd, $J = 1.4$, 1.6 Hz, 2H), 7.59 (s, 2H), 8.32 (d, $J = 3.6$ Hz, 2H). ^{13}C NMR (100 MHz, CDCl₃): δ 160.89, 146.25, 132.82, 126.16, 122.17, 115.48, 106.36, 46.65, 38.80, 31.90, 31.87, 31.48, 30.09, 29.62, 29.61, 29.54, 29.49, 29.32, 29.27, 26.48, 22.65, 22.63, 14.05. MS (MALDI-TOF, m/z): calcd for C₅₄H₈₈N₂O₄, 828.67; found, 828.53 (M).

Synthesis of 3,6-bis(5-bromofuran-2-yl)-2,5-bis(2-octyldodecyl)-pyrrolo[3,4-c]pyrrole-1,4(2H,5H)-dione (3)

To a 100 mL three neck flask equipped with a stirring bar, a condenser, and a dropping funnel were charged with **2** (4.5 g, 5.42 mmol) and chloroform (40 mL). Bromine (Br₂) (0.55 mL, 10.84 mmol) in chloroform (20 mL) was then added to the flask at room temperature through the dropping funnel. The mixture was stirred at room temperature overnight, then slowly poured into an aqueous solution of sodium thiosulfate and stirred for additional 30 min. The product was extracted with chloroform, then washed with DI water, and dried over anhydrous MgSO₄.

Removal of the solvent afforded the crude product which was further purified using column chromatography on silica gel (a mixture of hexane and chloroform as eluent) to give the product as a dark red solid (3.08 g, 58%). Mp (DSC): 105.0 °C. ^{1}H NMR (400 MHz, CDCl₃): δ 0.85 (t, $J = 6.2$ Hz, 12H), 1.10–1.40 (m, 64H), 1.76 (s, 2H), 3.96 (d, $J = 6.7$ Hz, 4H), 6.59 (d, $J = 3.4$ Hz, 2H), 8.27 (d, $J = 3.4$ Hz, 2H). ^{13}C NMR (100 MHz, CDCl₃): δ 160.87, 146.23, 132.78, 126.13, 122.14, 115.45, 106.34, 46.63, 38.78, 31.87, 31.84, 31.47, 30.07, 29.59, 29.52, 29.46, 29.29, 29.24, 26.46, 22.62, 14.02. MS (MALDI-TOF, m/z): calcd. for C₅₄H₈₆Br₂N₂O₄, 984.50; found, 986.38 (M + 2).

Synthesis of PDBFBT

To a 50 mL flask equipped with a condenser were charged **3** (0.2961 g, 0.3 mmol), 5,5′-bis(trimethylstannyl)-2,2′-bithiophene (0.1476 g, 0.3 mmol), and bis(triphenylphosphine)palladium(II) dichloride (7 mg, 0.01 mmol). After degassing and refilling argon for 3 times, toluene (20 mL) was added and the reaction mixture was raised to 90 °C and stirred for 48 h. To the reaction mixture was then added bromobenzene (0.5 mL) to react with the residual trimethylstannyl end group. The mixture was further stirred at 90 °C for 8 h before cooling down to room temperature. The mixture was then poured into stirring methanol (200 mL), filtered off, washed with methanol, and dried. The solid was then further purified by Soxhlet extraction using acetone (24 h), hexane (24 h), and then dissolved with chloroform. A blue solid was obtained. Yield: 0.294 g (98.7%). ^{1}H NMR (400 MHz, CDCl₃): δ 8.95 (br), 6.85 (br), 4.01 (br), 3.05 (br), 1.22 (br), 0.85 (br). GPC (at 40 °C; THF as eluent; polystyrene as standards): $M_n = 130\ 500$; $M_w/M_n = 2.27$. UV-vis-NIR: $\lambda_{max} = 770$ nm (chloroform); 776 nm (thin film). Anal. Calcd (%) for C₆₂H₉₀N₂O₄S₂: C 75.10, H 9.15, N 2.83, S 6.47; found: C 75.46, H 9.14, N 3.31, S 6.16. FT-IR: 3068, 2954, 2925, 2853, 1585, 1666, 1558, 1480, 1397, 1350, 1103, 1034, 790, 745, 733 cm^{-1}.

Fabrication and characterization of OTFT devices

PDBFBT was tested in OTFT devices with a top-contact, bottom-gate configuration, fabricated following a similar procedure as described in ref. 7. A heavily n-doped silicon wafer with a thermally grown silicon oxide (SiO₂) layer (~200 nm) having a capacitance of 17.25 nF cm^{-2} was used, wherein the wafer acts as the gate electrode and the SiO₂ layer acts as the gate dielectric. A solution of PDBFBT in chloroform (6 mg mL^{-1}) was filtered through a 0.2 μm syringe filter, and then spin-coated on the OTS-treated substrate at 1000 rpm for 60 s at room temperature. The polymer thin film (~30 nm in thickness) was annealed at 100, 150, and 200 °C, respectively, under nitrogen. Gold source/drain electrodes (~100 nm in thickness) were deposited on top of the polymer semiconductor layer by vacuum deposition through a shadow mask. The evaluation of transistor performance was carried out in a glove box filled with nitrogen using a Keithley 4200 SCS semiconductor characterization system.

The charge carrier mobility was calculated from the data in the saturated regime (gate voltage, V_{GS} < source-drain voltage, V_{SD}) according to the literature method.[7]

10834 | J. Mater. Chem., 2011, **21**, 10829–10835

This journal is © The Royal Society of Chemistry 2011

Acknowledgements

Notes and references

1 B. Tieke, A. R. Rabindranath, K. Zhang and Y. Zhu, *Beilstein J. Org. Chem.*, 2010, **6**, 830.

2 T. Beyerlein, B. Tieke, S. Forero-Lenger and W. Brütting, *Synth. Met.*, 2002, **130**, 115.

3 D. Cao, Q. Liu, W. Zeng, S. Han, J. Peng and S. Liu, *Macromolecules*, 2006, **39**, 8347.

4 L. Bürgi, M. Turbiez, R. Pfeiffer, F. Bienewald, H. Kirner and C. Winnewisser, *Adv. Mater.*, 2008, **20**, 2217.

5 Y. Li, *US Pat. Application* 2009/65766 A1, 2009 and 2009/0065878A1, 2009.

6 J. C. Bijleveld, A. P. Zoombelt, S. G. J. Mathijssen, M. M. Wienk, M. Turbiez, D. M. de Leeuw and R. A. J. Janssen, *J. Am. Chem. Soc.*, 2009, **131**, 16616.

7 Y. Li, S. P. Singh and P. Sonar, *Adv. Mater.*, 2010, **22**, 4862.

8 Y. Li, P. Sonar, S. P. Singh, M. S. Soh, M. van Meurs and J. Tan, *J. Am. Chem. Soc.*, 2011, **133**, 2198.

9 P. Sonar, S. P. Singh, Y. Li, M. S. Soh and A. Dodabalapur, *Adv. Mater.*, 2010, **22**, 5409.

10 M. M. Wienk, M. Turbiez, J. Gilot and R. A. J. Janssen, *Adv. Mater.*, 2008, **20**, 2256.

11 E. Zhou, S. Yamakawa, K. Tajima, C. Yang and K. Hashimoto, *Chem. Mater.*, 2009, **21**, 4055.

12 Y. Zou, D. Gendron, R. Neagu-Plesu and M. Leclerc, *Macromolecules*, 2009, **42**, 6361.

13 L. Huo, J. Hou, H. Chen, S. Zhang, Y. Jiang, T. L. Chen and Y. Yang, *Macromolecules*, 2009, **42**, 6564.

14 A. P. Zoombelt, S. G. J. Mathijssen, M. G. R. Turbiez, M. M. Wienk and R. A. J. Janssen, *J. Mater. Chem.*, 2010, **20**, 2240.

15 J. C. Bijleveld, V. S. Gevaerts, D. D. Nuzzo, M. Turbiez, S. G. J. Mathijssen, D. M. de Leeuw, M. M. Wienk and R. A. J. Janssen, *Adv. Mater.*, 2010, **22**, E242.

16 S. Andoa, A. Nishida, E. Fujiwara, H. Tadab, Y. Inoue, S. Tokito and Y. Yamashita, *Synth. Met.*, 2006, **156**, 327.

17 T. Minari, Y. Miyata, M. Terayama, T. Nemoto, T. Nishinaga, K. Komatsu and S. Isoda, *Appl. Phys. Lett.*, 2006, **88**, 083514.

18 O. Gidron, A. Dadvand, Y. Sheynin, M. Bendikov and D. F. Perepichka, *Chem. Commun.*, 2011, **47**, 1976.

19 T.-L. Choi, K.-M. Han, J.-I. Park, D.-H. Kim, J.-M. Park and S. Lee, *Macromolecules*, 2010, **43**, 6045.

20 C. H.Woo, P. M. Beaujuge, T. W. Holcombe, O. P. Lee and J. M. J. Fréchet, *J. Am. Chem. Soc.*, 2010, **132**, 15547.

21 J. C. Bijleveld, B. P. Karsten, S. G. J. Mathijssen, M. M. Wienk, D. M. de Leeuw and R. A. J. Janssen, *J. Mater. Chem.*, 2011, **21**, 1600.

22 U. Salzner, J. B. Lagowski, P. G. Pickup and R. A. Poirier, *Synth. Met.*, 1998, **96**, 177.

23 *Handbook of Liquid Crystals*, ed. D. Demus, J. W. Goodby, G. W. Gray, H. W. Spiess and V. Vill, Wiley-VCH, Weinheim, Germany, 1998.

24 H. Sirringhaus, P. J. Brown, R. H. Friend, M. M. Nielen, K. Bechgaard, B. M. W. Langeveld-Voss, A. J. H. Spiering, R. A. J. Janssen, E. W. Meijer, P. Herwig and D. M. de Leeuw, *Nature*, 1999, **401**, 685.

25 B. S. Ong, Y. Wu, Y. Li, P. Liu and H. Pan, *Chem.–Eur. J.*, 2008, **14**, 4766.

26 I. McCulloch, M. Heeney, C. Bailey, K. Genevicius, I. Macdonald, M. Shkunov, D. Sparrowe, S. Tierney, R. Wagner, W. M. Zhang, M. L. Chabinyc, R. J. Kline, M. D. McGehee and M. F. Toney, *Nat. Mater.*, 2006, **5**, 328.

27 Y. Li, Y. Wu, P. Liu, M. Birau, H. Pan and B. S. Ong, *Adv. Mater.*, 2006, **18**, 3029.

28 H. Pan, Y. Li, Y. Wu, P. Liu, B. S. Ong, S. Zhu and G. Xu, *J. Am. Chem. Soc.*, 2007, **129**, 4112.

29 A. R. Brown, C. P. Jarrett, D. M. de Leeuw and M. Matters, *Synth. Met.*, 1997, **88**, 37.

30 C. D. Dimitrakopoulos, S. Purushothaman, J. Kymissis, A. Callegari and J. M. Shaw, *Science*, 1999, **283**, 822.

31 G. Horowitz, R. Hajlaoui, D. Fichou and A. ElKassmi, *J. Appl. Phys.*, 1999, **85**, 3202.

32 G. Horowitz, M. E. Hajlaoui and R. Hajlaoui, *J. Appl. Phys.*, 2000, **87**, 4456.

33 K. Kima, M. K. Kima, H. S. Kanga, M. Y. Choa, J. Joo, J. H. Kimb, K. H. Kimb, C. S. Hongb and D. H. Choi, *Synth. Met.*, 2007, **157**, 481.

34 Y. Kimura, M. Niwano, N. Ikuma, K. Goushi and K. Itaya, *Langmuir*, 2009, **25**, 4861.

35 S. Braun, W. R. Salaneck and M. Fahlman, *Adv. Mater.*, 2009, **21**, 1450.

36 J. Rivnay, M. F. Toney, Y. Zheng, I. V. Kauvar, Z. Chen, V. Wagner, A. Facchetti and A. Salleo, *Adv. Mater.*, 2010, **22**, 4359.

37 W. Zhang, J. Smith, S. E. Watkins, R. Gysel, M. McGehee, A. Salleo, J. Kirkpatrick, S. Ashraf, T. Anthopoulos, M. Heeney and I. McCulloch, *J. Am. Chem. Soc.*, 2010, **132**, 11437.

38 U. H. F. Bunz, *Angew. Chem., Int. Ed.*, 2010, **49**, 5037.

39 (*a*) M. S. A. Abdou, F. P. Orfino, Y. Son and S. Holdcroft, *J. Am. Chem. Soc.*, 1997, **119**, 4518; (*b*) C.-K. Lu and H.-F. Meng, *Phys. Rev. B: Condens. Matter Mater. Phys.*, 2007, **75**, 235206; (*c*) H.-H. Liao, C.-M. Yang, C.-C. Liu, S.-F. Horng, H.-F. Meng and J.-T. Shy, *J. Appl. Phys.*, 2008, **103**, 104506.

40 B. S. Ong, Y. Wu, P. Liu and S. Gardner, *J. Am. Chem. Soc.*, 2004, **126**, 3378.

41 (*a*) Y. Li, J. Ding, M. Day, Y. Tao, J. Lu and M. D'iorio, *Chem. Mater.*, 2004, **16**, 2165; (*b*) D. M. Leeuw, M. M. J. Simenon, A. R. Brown and R. E. F. Einerhand, *Synth. Met.*, 1997, **87**, 53; (*c*) Y. Cui, X. Zhang and S. A. Jenekhe, *Macromolecules*, 1999, **32**, 3824.

42 Y. Wei, Y. Yang and J.-M. Yeh, *Chem. Mater.*, 1996, **8**, 2659.

This journal is © The Royal Society of Chemistry 2011

J. Mater. Chem., 2011, **21**, 10829–10835 | 10835